

# PHOTGRAMMETRIC PROCESSING AND FRUITION OF PRODUCTS IN OPEN-SOURCE ENVIRONMENT APPLIED TO THE CASE STUDY OF THE ARCHAEOLOGICAL PARK OF POMPEII

I. Ferrando<sup>1,\*</sup>, E. Berrino<sup>1</sup>, B. Federici<sup>1</sup>, S. Gagliolo<sup>1</sup>, D. Sguerso<sup>1</sup>

<sup>1</sup>Geomatics Laboratory, Department of Civil, Chemical and Environmental Engineering (DICCA), University of Genoa, via Montallegro 1, 16145 Genoa, Italy – (ilaria.ferrando, sara.gagliolo)@edu.unige.it, (bianca.federici, domenico.sguerso)@unige.it

## Commission IV, WG IV/4

**KEY WORDS:** Integrated geomatic survey, Archaeological site, Point clouds, Orthophotos, “Master/slave” GIS environment, Open-source software.

## ABSTRACT:

The paper presents the geomatic survey campaign carried out in the Domus V of Pompeii Archaeological site, the photogrammetric processing of the collected images and the following fruition of the deriving products deploying open-source software. Among all the produced results, the orthophotos of the vertical walls of one of the Domus V rooms are made available through a “master/slave” GIS environment, where each orthophoto is uploaded in a “slave” project whose visualization is triggered by querying the corresponding geometry representing the wall in the “master” project. This strategy allows to include the display of the third dimension, i.e., the altimetric one, within a traditional GIS environment, so to constitute a 3D GIS representation. This is particularly useful to realize a catalogue of all the archaeological site in the future to be viewed, queried and exploited also by non-specialists in geomatics or archaeology fields of knowledge.

## 1. INTRODUCTION

The Geomatics surveying in Cultural Heritage and, more specifically, in Archaeology contexts has widely spread in the last years for preservation purposes, thanks to the reachable high accuracy and the reliability of the final products, the possibility of extracting both metric and thematic information, and the easy management and integration of the entire workflow. Indeed, the interdisciplinary approach, involving both Cultural Heritage and Geomatics fields of knowledge, can represent a fruitful occasion to better focus on the documentation and representation of Cultural Heritage in view of its enhancement, restoration and protection (Tsiafaki and Michailidou, 2015; Bitelli et al., 2017; Girelli et al., 2019). In this context, the Geomatics expertise is highly requested for the generation of 2D and 3D digital products, mainly thanks to the laser scanning and the 3D imaging techniques, i.e., photogrammetry, even from Uncrewed Aerial vehicles (UAV).

The focus of the present paper is situated in the Archaeological Park of Pompeii, that has been widely studied in recent years (Monego et al., 2019; Francolini et al., 2020; Verde, 2020; Autelitano et al., 2022; Barba et al., 2022). Here, the Domus V (Regio VII, Insula 14) represents the case study to present and discuss the geomatic strategy for the survey campaign, data processing and product fruition in an archaeological context. The site was surveyed in September 2020 by the Geomatics Laboratory of Genoa University in collaboration with the archaeologist group of the same University, under the ministerial concession DG 553 Class 34.31.07/246.7 of 26 January 2016 and its renewal on 9 April 2019 (34.31.07/3.4.7/2018). The survey campaign involved several integrated geomatic techniques: UAV and terrestrial photogrammetry, and laser scanner, framed in the same system thanks to temporary Ground Control Points (GCPs), surveyed with GNSS (Global Navigation Satellite Sys-

tem) in Network Real Time Kinematic (NRTK) positioning strategy. The integrated survey was planned, designed and realized so to allow to move from a general view of the entire site to an increasingly detailed one, mainly aimed at the vertical walls, thanks to the global framing provided by the UAV survey. The UAV and terrestrial photogrammetry campaigns were processed through the open-source software MicMac (Rupnik et al., 2017) to create the dense point clouds, and CloudCompare, ver. 2.11.3 (2022) to align the different blocks. MicMac was chosen for its open-sourceness and its rigorousness in the photogrammetric processing, both related to the estimation of the external/internal orientation parameters and the dense matching to obtain the 3D point clouds from the images, that is based on a multi-scale, multi-resolution pyramidal approach that minimizes the outliers and the noise. Due to the not linear computational time in respect of the number of images, the MicMac processing was split in blocks of 500 images each (about 24 hours of processing time), with 100 overlapping images between two consecutive blocks, to align them through a point-to-point strategy. The obtained 3D point cloud was oriented and scaled using 15 natural points found on the terrestrial laser scanner point cloud, obtaining deviations on points positions ranging between 1 and 2 cm. The quality of the alignment was tested computing the distance between the laser scanner and the photogrammetric point clouds using CloudCompare M3C2 algorithm (Lague et al., 2013) on a representative area of 1.60 m × 2.25 m of the fresco on the central wall of the surveyed room, obtaining distances of ±5 mm orthogonally to the wall. Moreover, the software MAGO (Gagliolo et al., 2019a,b; Gagliolo, 2021), developed in C++ environment within the Geomatics Laboratory, was used to produce high-resolution orthophotos of vertical walls. The produced orthophotos were made accessible and viewable via a QGIS project (QGIS Development Team, 2022) built so to manage two different reference frames, i.e., the traditional planimetric plane (X,Y)

\* Corresponding author

and the vertical plane of the walls (X-Y,Z), where the X-Y represent the planimetric coordinates along the wall direction. This allows to introduce the third dimension in the typical GIS representation, thus realizing a 3D GIS environment. The QGIS project is organized with a “master/slave” architecture, where the master project is dedicated to the (X,Y) plane and reports the vectorial geometries (lines) representing the perimeter of the walls, whereas a different slave project is dedicated to each specific wall with the corresponding orthophoto in a (X-Y,Z) plane. Each slave project is connected to the master thanks to a QGIS action that opens it when clicking on the corresponding wall in the master project. In each sub-project, the orthophoto of the wall is displayed together with three default shapefiles: point, line and polygon, respectively. Moreover, QGIS was employed to perform the orthophoto classification based on the state of conservation of the wall, i.e., crumbling, degraded, good conditions, preserved, through user-defined training areas, from which the spectral signatures to be used in the supervised classification are computed. Thanks to the “nested” GIS environment, the ensemble of the produced orthophotos can be viewed and linked to the corresponding geometry, forming a catalogue for an overall analysis of the entire archaeological site, taking advantage of an increasingly detailed and precise zooming in the areas of interest. This environment can also be used by non-expert geomatics users, making the survey products available for analysis in different specific disciplines.

The paper is organized as follows: section 2 describes the case study (2.1) and the integrated geomatic survey (2.2), focusing on the strategy adopted to optimize the logistics and timing of the operations; section 3 is related to photogrammetric data processing (3.1), from their collection, elaboration and integration to the realization of orthophotos (3.2); finally, section 4 deals with the fruition of the orthophotos within the GIS environment and their classification based on the state of conservation of the walls. The conclusions highlight the adopted survey strategy, the performance of the employed software and their functions to obtain the required results.

This work constitutes an example of the application of Geomatics into archaeology field of knowledge for the specific case study, even if all the proposed and discussed procedures can be considered applicable to any context in a multidisciplinary perspective.

## 2. INTEGRATED SURVEY

In the following, the case study and the integrated geomatic survey campaign strategy are described, in sections 2.1 and 2.2, respectively.

### 2.1 Case study

The analyzed case study is Domus V, also known as the “House of the Queen of England”, located in Regio VII, Insula 14 (represented as a map in Figure 1) of the Archaeological park of Pompeii (Naples, Italy). The site covers an area of approximately 60 m × 35 m and it is constituted by three domus and twelve shops overlooking Via dell’Abbondanza, the most important artery of the city. Domus V, depicted in Figure 2, is an atrium domus consisting of 27 rooms. The presence of secondary elements such as staircases and gutters suggests the possibility that the building had several floors in ancient times (Capobianco et al., 2021; Capobianco and Gagliolo, 2022 (in press)).



Figure 1. Map of Regio VII, Insula 14.



Figure 2. Aerial image of Domus V.

### 2.2 Integrated survey campaign

The integrated geomatic survey campaign of Domus V took place on 22–24 September 2020, under concession DG 553 Class 34.31.07/246.7 of 26 January 2016 and its renewal on 9 April 2019 (34.31.07/3.4.7/2018) by MiC (Italian Ministry of Culture, formerly MiBACT).

The employed survey technologies include:

1. UAV photogrammetry through a DJI Mavic 2 Pro drone with a 20 MPx Hasselblad L1D-20c camera. Two nadir surveys were carried out at 15 and 40 m AGL (above ground level) flight height, respectively. An additional survey with a tilting angle of 45° at a flight altitude of 15 m was performed along concentric paths around the site. In all the UAV surveys, the forward and side image overlappings were set to 80% and 60%, respectively. A total of 1400 photos were taken; for the datasets with a flight altitude of 40 m the GSD (Ground Sample Distance), i.e., the size of the pixel on the ground, was 10 mm, while for those with a flight altitude of 15 m the GSD was 4 mm. The photogrammetric surveys are framed thanks to temporary GCPs, surveyed with GNSS in Network Real Time Kinematic (NRTK) positioning strategy.
2. Terrestrial photogrammetry through a Canon Eos 40D camera with focal length of 17 mm. About 7000 images of the internal vertical walls of Domus V were taken at a shooting distance of about 2 m following a bottom-to-top

trajectory. This setting guarantees a complete and highly-detailed survey, with a GSD equal to 0.7 mm.

3. Terrestrial laser scanning, using the Z+F 5006h phase difference instrument. A total of 26 scans, one for each room constituting the Domus V, was performed in super high resolution, corresponding to 20000 points/360°.
4. GNSS and Total Station to detect the GCPs. For the GNSS positioning, the Topcon Hiper Pro instrument was used, and the survey was carried out in NRTK mode in connection with the positioning service of the Campania Region. The employed Total Station employed was the Leica TCR703.

A preliminary survey was performed to state the situation of the site and the possible deriving operative conditions. It emerged a substantial absence of both vegetation cover and other significant obstacles; this led to an excellent satellite visibility for GNSS positioning and an easy UAV flight planning. The survey strategy was designed so to optimize the time of placing and surveying GCPs, which is notoriously a time consuming operation. It should be noted that the site was open to the public during the survey campaign, so the UAV survey was carried out very early in the morning, before the opening time. The GNSS and Total Station surveys were conducted when the visitors were present, so a special care was paid to not constrain the visits too much; this was one of the most demanding activities, given the logistics of all the equipment. The laser scanner survey was conducted in areas closed to the public, therefore it did not present any difficulties.

The adopted strategy consisted in an integrated survey deploying various techniques so to describe the whole site of interest from a general view to an increasingly detailed one, taking advantage of the possibility of linking the several datasets thanks to the unique frame given by the GCPs. Indeed, the UAV photogrammetry, framed thanks to GNSS and Total Station, gives a general view of the site, whereas a highly-detailed description of the vertical walls is given by the terrestrial photogrammetry, which is framed in the laser scanner survey, in turn framed in the UAV survey.

Figure 3 depicts the survey schema, where the different colored boxes represent the areas surveyed by UAV at 40 m AGL, by UAV at 15 m AGL and by terrestrial photogrammetry and laser scanner in red, green and light blue, respectively. The yellow dots represent GCPs, measured with both GNSS and Total Station. The red circle highlights the room in which the photogrammetric processing is focused (section 3.1). The first phase of the survey concerned the entire Insula 14, involved UAV photogrammetry at 40 m and 15 m AGL and lasted about a couple of hours. The UAV survey allowed the global framing of the laser scanner scans, which otherwise would have been difficult to be registered due to issues related to arranging targets in a way that two consecutive scans have at least three common targets, also considering the impossibility of applying anything on the walls, even for limited time. The laser scanning of the 27 rooms took about 8 hours.

### 3. DATA PROCESSING AND RESULTS

The data processing strategies and the corresponding obtained products are here described for photogrammetry and the integration of the point clouds resulting from laser scanner and photogrammetry (section 3.1) and for the orthophoto generation (section 3.2). As already mentioned, the data elaboration is focused on the room highlighted in the red circle in Figure 3.



Figure 3. Schema of integrated survey campaign. UAV photogrammetry at 40 m AGL was performed over red areas, UAV photogrammetry at 15 m AGL was conducted over green areas, whereas laser scanning and terrestrial photogrammetry surveyed the light blue areas, respectively. The red circle represents the room where the data processing is focused.

All the following described processing were performed using a pc with an Intel Core i7-8750H processor, 16 GB of RAM and a GeForce GTX 1050 4 GB dedicated video card.

#### 3.1 Photogrammetric data processing

The images deriving from the UAV surveys were processed through the open-source software MicMac, developed by the MATIS laboratory of the French National Geographical Institute (IGN). MicMac is capable of completing the entire photogrammetric processing, producing the dense point cloud as final output. MicMac was chosen for its open-sourceness and its rigorousness in the photogrammetric processing, related to both the estimation of the external/internal orientation parameters and the dense matching to obtain the 3D point clouds from the images, based on a multi-scale, multi-resolution pyramidal approach that minimizes the outliers and the noise. Moreover, MicMac uses rigorous photogrammetric methodologies to compute the external orientation parameters, takes into account the internal orientation parameters of the optics, and uses the calibration models of digital photogrammetry to perform the auto-calibration. The photogrammetric processing can be summarized as follows: (1) tie points extraction; (2) camera positions estimation; (3) 3D point cloud generation through dense matching algorithm. The approach followed by this algorithm allows to limit the search for combinations: in the initial step, the search window in the master image (patch) is first identified and the entire depth range is explored. In the following steps, the area to be explored is derived from the previous step (for each hypothetical 3D point) and the result of the correlation is computed. For each level, the correlation result is projected into the neighbouring images and the final value is derived using a global likelihood function. Thanks to an energy minimization approach, the process will also minimize the outliers and the noise of the extracted point cloud. At the end of the processing, a depth image is produced from which the 3D point cloud is derived by extracting the elevation for each point, whereas the radiometric tone is obtained from the oriented images. As previously outlined, MicMac optimizes the search for tie points if a well-defined geometry is present, e.g., a strip of images. In the present case, the search for matches was limited within 20 adjacent images. Datasets composed by different number of images were processed to state the processing times in view

of optimizing the elaboration. The obtained processing times were about 6, 24 and 52 hours, for datasets composed by 100, 500 and 1000 images, respectively. Given the good compromise between the number of processed images and the time, it was decided to carry out the processing dividing the entire dataset in blocks of 500 images each, considering 100 common images between consecutive blocks to correctly align them in the following. Figure 4 reports two point clouds generated from two blocks of 500 images, highlighting the overlapping parts (obtained from 100 images) in the red circles.

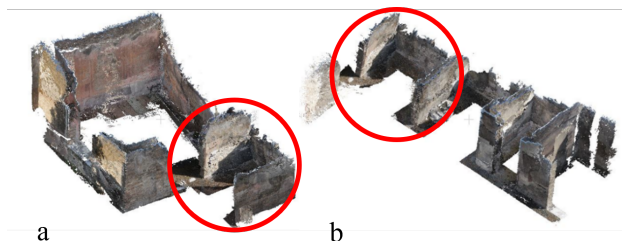


Figure 4. Two point clouds (a) and (b) deriving from two blocks of images and the common overlapping part (in the red circles).

The point clouds were scaled using GCPs coordinates detected from natural points of the laser scanner point cloud, extracted using the free and open-source software CloudCompare. Through the MicMac command *mm3d SaisieAppuisInitQT*, the GCPs were digitized in the images. This command requires as input the sequence of images on which to digitize the GCPs and a text file listing the points and their coordinates; it returns as output a *.xml* file of the points and coordinates to be used as input in the next *mm3d GCPBascule* command to apply the proper roto-translation and scale to the point clouds. It should be pointed out that *mm3d SaisieAppuisInitQT* does not handle a large number of images, so it was necessary to run it several times by partitioning the entire sequence of images, saving all to the same file, so to finally have a single general *.xml* output file. Figure 5 reports the selected GCPs on the laser scanner and photogrammetric point clouds, on the left and on the right, respectively.

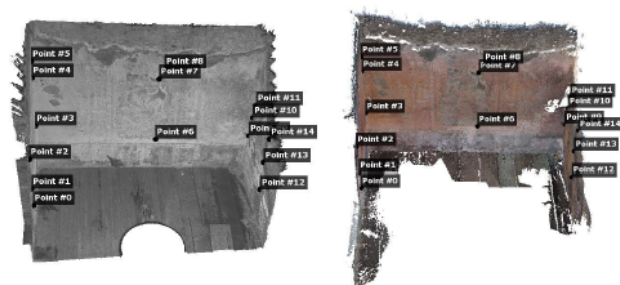


Figure 5. GCPs chosen on the laser scanner point cloud (on the left) and corresponding points on the photogrammetric point cloud (on the right).

A total of 15 points were taken: three on the left wall, three on the left corner, three on the central wall (fresco), three on the right corner and three on the right wall. The residuals, reported in Table 1, were computed to assess the quality of the process. As Table 1 shows, the residuals range between 1 and 2 cm, with the only exception of GCP 6 that has a considerably high deviation. To further improve the result, CloudCompare was used to align the photogrammetric point cloud on the laser scanner one

| GCP number | Residual [mm] |
|------------|---------------|
| 0          | 18            |
| 1          | 13            |
| 2          | 13            |
| 3          | 5             |
| 4          | 12            |
| 5          | 11            |
| 6          | 45            |
| 7          | 18            |
| 8          | 23            |
| 9          | 12            |
| 10         | 13            |
| 11         | 17            |
| 12         | 13            |
| 13         | 3             |
| 14         | 23            |

Table 1. GCPs residuals.

and then to compute the distance between the two point clouds by the CloudCompare M3C2 algorithm (Lague et al., 2013). This algorithm computes signed distances between two point clouds selecting a set of “core” points from the reference point cloud (the laser scanner cloud) along the normal direction, i.e., orthogonally to the plane defined by the neighboring points of each core point, towards the compared point cloud (the photogrammetric point cloud). This test, performed on a representative area of 1.60 m × 2.25 m on central wall fresco to assess the quality of the point clouds alignment, shows that the average distance between the two clouds ranges between ±5 mm.

### 3.2 Orthophotos generation

An orthophoto is a metrically correct and georeferenced image on which measurements can be taken. If the performed measurements are multiplied by the orthophoto scale factor, the actual measurements of the object are obtained. In order to generate an orthophoto it is necessary to have the image to be orthorectified and a Digital Surface Model (DSM). Nowadays, most of the photogrammetric software can generate orthophotos by using a mesh. On the one hand, this produces a high degree of detail, comparable with the GSD value; on the other hand, it introduces an approximation in the description of the object, due to the simplified method used to generate the polygons of the mesh. To overcome this second aspect, the software MAGO (Adaptive Mesh for Orthophoto Generation) was employed. It consists of about 3500 lines of code implemented in C++ environment, together with a simple Graphical User Interface (GUI) realized in Qt. It exploits the contribution of the open source library OpenCV, which contains many functions for both matrices and images management. It requests the point cloud and the external and internal orientation (EO and IO) parameters as inputs, then it considers a best-fitting triangular plane area where the image pixel is projected at its original resolution. The five working steps are described below:

1. definition of the orthophoto plane;
2. acquisition of the IO and EO parameters of the image;
3. definition of orthophoto dimensions and resolution and creation of a supportive reference system, whose XY plane is parallel to the orthophoto plane, so that the real visibility of points is easily understandable based on Z coordinate;
4. iterative process to determine the three points in the plane where the collinearity ray and the point cloud intersect. Each face of the mesh is generated directly from the point cloud without further simplification or resampling, thus, the adaptive mesh is at the highest possible resolution;

- projection of the color of each pixel in the image onto the orthophoto map.

Further details on MAGO can be found in Gagliolo et al. (2019a). MAGO was recently updated to generate orthophotos of non-coplanar adjacent walls, i.e., forming an edge, through a rotation so that the two walls are placed in a continuous common plane. Figure 6 represents the perspective view of two adjacent walls (upper part) and the corresponding single and joint orthophotos produced by MAGO.

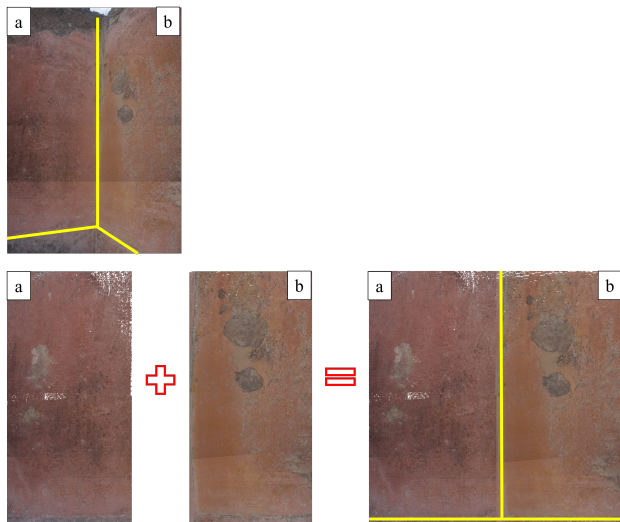


Figure 6. Perspective view and corresponding orthophotos of two adjacent walls.

#### 4. FRUITION IN GIS ENVIRONMENT

For the fruition of the produced orthophotos, a QGIS project capable of including both planimetric spatial information and data with altimetric distribution was realized. Indeed, GIS software typically display and manage planimetric data, to which the third dimension, i.e., the elevation, can be associated as an attribute of the object of known planimetric position. In this work, a 2D+1 GIS environment of a Domus V room was created, as shown in Figure 7: the cube of the room on the left, that shows in 3D the considered walls, was expanded into three 2D surfaces. The green axes, labelled as  $x$  and  $y$ , represent the 2D horizontal and vertical axes (relative to a specific wall) on which each orthophoto is projected.

This was realized through a master/slave architecture of QGIS projects, so to manage two different reference frames: the traditional planimetric plane ( $X, Y$ ) and the vertical plane of the walls ( $X, Y, Z$ ), where the  $X, Y$  represent the planimetric coordinates along the wall direction. The master project is dedicated to the ( $X, Y$ ) plane and reports the vectorial geometries (polylines) representing the perimeter of the walls. A different slave project is dedicated to each specific wall with the corresponding orthophoto in a ( $X, Y, Z$ ) plane. Each slave project is connected to the master thanks to a QGIS action that opens it when clicking on the corresponding wall in the master project. Another QGIS action is defined in the master project, just for visualization purposes of the corresponding orthophoto. Both the actions are triggered by clicking on a side of the room in the master project. To be more precise, the first recorded action is an “Open URL” QGIS action type, with the task of opening the

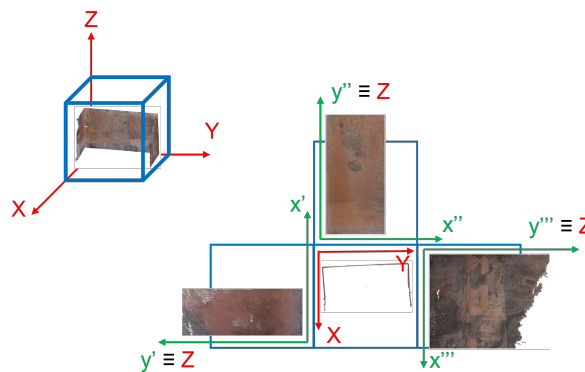


Figure 7. Developing of 3D virtual model of the walls into three 2D surfaces.

object described in a specific column of the shapefile attribute table, i.e., the “Image” field containing the orthophoto path of each side of the room. The second action is a “Windows” QGIS action type that triggers the opening of a slave QGIS project once a section of the polyline representing a wall in the master project is clicked. In each slave project, the orthophoto of the wall is displayed together with three default shapefiles: point, line and polygon. The attribute tables of the three shapefiles are set to be automatically updated once the user introduces a new geometry. In particular, the point shapefile returns the coordinates of a clicked point both in image ( $x, y$ ) coordinates (converted from pixel units in meters) and object coordinates ( $X, Y$ ), referring to the external reference system, where  $X$  is the UTM planimetric coordinate, while  $Y$  is the geometric height of the wall, i.e.,  $Z$  in a 3D system. The following relations are used to convert the image coordinates ( $x, y$ ) from pixels to meters:

$$x = \frac{\$x \cdot GSD}{10^3}; y = \frac{\$y \cdot GSD}{10^3}, \quad (1)$$

where  $x$  and  $y$  are the image coordinates (in meters units),  $\$x$  and  $\$y$  are the automatically computed  $x$  and  $y$  coordinates (in pixel units), and  $GSD$  is the Ground Sample Distance, equal to 2 mm/pixel in the present case. To compute  $X$  in the external reference system, i.e., ETRF2000-2008.0 reference system with UTM projection in zone 33N, the azimuth of the wall ( $\alpha$ ), i.e., its orientation with respect to an horizontal axis, and the  $X$  coordinate of the first point of the wall ( $X_i$ ), i.e., the one with the lowest east coordinate, are taken into account:

$$X = \frac{\$x \cdot GSD \cdot \cos(\alpha)}{10^3} + X_i, \quad (2)$$

The values of  $\alpha$  and  $X_i$  should be computed by the user in the master project and substituted with the corresponding values in the automatically implemented relations before drawing the points. As already mentioned, the  $Z$  coordinate corresponds to the height of the wall, and it can be obtained as follows:

$$Z = \frac{\$y \cdot GSD}{10^3} \quad (3)$$

In the line shapefile, the length  $L$  of the line, that the user can trace, is automatically computed as:

$$L = \$length \cdot \frac{GSD}{10^3}, \quad (4)$$

where \$length is the QGIS command to automatically return the ellipsoidal length of a line. Finally, for the polygon shapefile, the area A (in square meters) and the perimeter p (in meters) of the drawn shape are automatically computed as:

$$A = \frac{GSD \cdot GSD}{10^6}; p = \frac{\$perimeter \cdot GSD}{10^3} \quad (5)$$

where \$perimeter is the QGIS command to compute the ellipsoidal perimeter of a polygon shapefile.

An additional feature of the slave QGIS project is the possibility of performing the orthophoto supervised classification based on the state of conservation of the wall, i.e., crumbling, degraded, good conditions, preserved, through user-defined training areas (Figure 8a). Once the training areas have been drawn, they are converted to raster format based on their category: categories 1–4 correspond to increasing state of conservation of the wall. The spectral signatures were then created using the *i.gensig* command, then the *i.maxlik* module was used to classify the orthophoto, obtaining the results shown in Figure 8b.

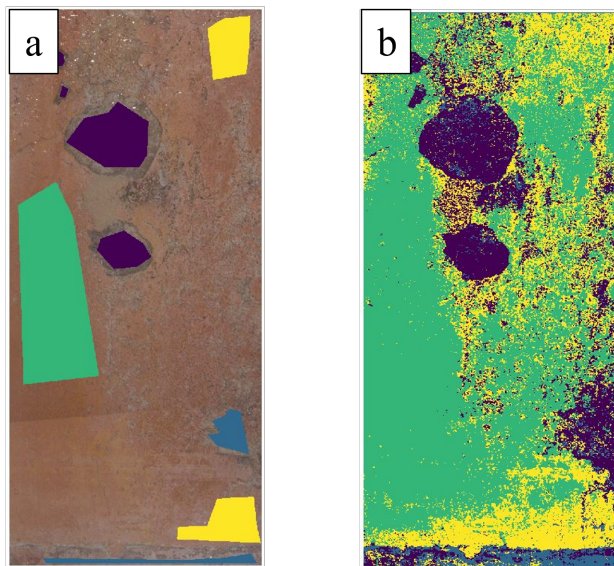


Figure 8. Training areas (a) and resulting classification of orthophoto (b) based on the state of conservation of the wall, obtained with supervised image classification.

Performing a report on the classified image, the area and percentage of each class is computed, to quantify the area of the wall pertaining to each class, as Table 2 reports.

| Class number | Description     | Area [m <sup>2</sup> ] | Cover [%] |
|--------------|-----------------|------------------------|-----------|
| 1            | Crumbling       | 0.433                  | 17.19     |
| 2            | Degraded        | 0.124                  | 4.94      |
| 3            | Good conditions | 1.344                  | 53.35     |
| 4            | Preserved       | 0.618                  | 24.52     |

Table 2. Area and percentage cover pertaining to each class.

The last operation set to be carried out within QGIS environment is the possibility to check the verticality of the wall by analyzing its DSM. The DSM of the analysed wall was generated with the *Rasterize* function of CloudCompare, with a pixel resolution of 1 cm, and then imported in the corresponding slave QGIS project. An example of this analysis is shown in Figure 9: the maximum difference in the direction orthogonal to the DSM wall plane was evaluated as about 10 cm; indeed

the color scale, representing the heights of the wall orthogonally to the (x'',y'') plane, ranges from 0 (blue color) to 100 (red color) mm.

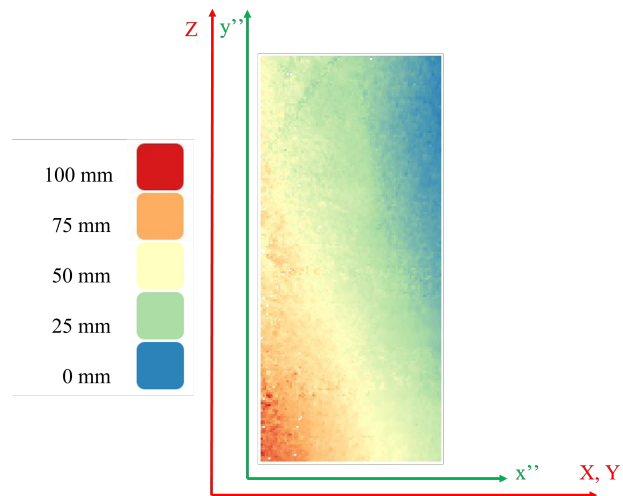


Figure 9. Deviation of the wall from vertical.

## 5. CONCLUSIONS AND FUTURE PERSPECTIVES

This work is aimed to address the contribution of Geomatics in Archaeology field of knowledge, by making available state-of-the-art surveying and processing techniques, with innovative approaches also for the visualization and analysis of the obtained results in a GIS environment. The identified techniques and strategies have been applied to the case study of Regio VII, Insula 14, Domus V of the Archaeological Park of Pompeii (Naples, Italy), that was surveyed in September 2020. For this specific case, a particular integrated survey strategy was adopted in order to optimize the timing and logistics of the equipment due to the crowding of the site. Given that the main objective was to obtain a survey with a high degree of detail of the vertical walls only, the integration of these techniques allowed the framing of this survey within the overall survey of the entire site area.

The post-processing of data was carried employing several free and open-source software: MicMac for the photogrammetric processing, CloudCompare to check the quality of the obtained photogrammetric point cloud through the comparison with the laser scanner-derived and to compute the DSM of the considered vertical walls, and QGIS to allow the fruition of orthophotos and to analyze the state of conservation of the walls. The orthophotos of the vertical walls were generated by MAGO application (Adaptive Mesh for Orthophoto Generation), to realize high-resolution orthophotos on self-adaptive reference planes even in the presence of developments with different orientation, e.g., corner walls. As already stated, the produced orthophotos were made available within a “nested” GIS environment, building a master/slave strategy of QGIS project. A slave project dedicated to visualize and measure the orthophoto of a room wall is opened by clicking on the geometry representing the planimetric position of that wall in the master project. In this way, the GIS environment is able to treat both the planimetric spatial information and the altimetric one, through the direct visualization of the orthophotos of the walls. In addition to displaying the wall, the slave project contains three default shapefiles (point, polyline and polygon) that allow to perform

measurements on the orthophoto. Finally, the image classification of orthophotos based on the state of conservation of the wall and the evaluation of the deviation of the wall with respect to the vertical were performed.

Thanks to this “nested” GIS environment, the ensemble of the produced orthophotos can be viewed and linked to the corresponding geometry, forming a catalogue for an overall analysis of the entire archaeological site, taking advantage of an increasingly detailed and precise zooming in the areas of interest. This environment can also be used by non-expert geomatics users to make use of the survey products for further analysis.

In the future, it will be possible to carry out the analysis scheme, here reported and referred to a single wall, to all the vertical developments of the site, bringing together all the results in a single database of the entire project. In this way it will be possible to carry out an overall analysis of the entire site and make it available to experts in other specific disciplines, in order to obtain an increasingly detailed and precise project in the various areas of interest.

### ACKNOWLEDGEMENTS

The authors wish to thank: Prof. Silvia Pallecchi, Associate Professor in Archaeological Research Methodologies at University of Genoa; Dr. Alice Capobianco, graduated at the School of Specialization in Archaeological Heritage of University of Genoa; the staff of the Archaeological Park of Pompeii. This project has been developed under the concession DDG 553 34.31.07/246.7 of 26 January 2016 and its renewal 34.31.07/3.4.7/2018 of 9 April 2019.

### REFERENCES

Autelitano, F., Bruno, N., Martinelli, R., Calvanese, V., Garilli, E., Biancardo, S., Dell’Acqua, G., Veropalumbo, R., Zerbi, A., Roncella, R., Giuliani, F., 2022. The construction of a street never opened to traffic. The extraordinary discovery of pavement engineering in vicolo dei Balconi of Pompeii. *Journal of Cultural Heritage*, 54, 108–117. <https://doi.org/10.1016/j.culher.2022.01.012>.

Barba, S., Benedetto, A. D., Fiani, M., Gujski, L., 2022. A method to improve the accuracy of sparse UAV point cloud applied to the Amphitheater of Pompeii. *Journal of Physics: Conference Series*, 2204(1). <https://doi.org/10.1088/1742-6596/2204/1/012081>.

Bitelli, G., Balletti, C., Brumana, R., Barazzetti, L., D’Urso, M., Rinaudo, F., Tucci, G., 2017. Metric documentation of cultural heritage: research directions from the Italian GAMHer project. *The International Archives of the Photogrammetry, Remote Sensing and Spatial Information Sciences*, XLII-2/W5, 83–90. <https://doi.org/10.5194/isprs-archives-XLII-2-W5-83-2017>.

Capobianco, A., Gagliolo, S., 2022 (in press). Applicazione del rilevamento geomatico alla Domus della Regina d’Inghilterra a Pompei (VII, 14, 5): risultati preliminari. *Archeologia e Calcolatori*, 33(1), 17–34. <https://doi.org/10.19282/ac.33.1.2022.00>.

Capobianco, A., Gagliolo, S., Pallecchi, S., Sguerso, D., 2021. Analysis of historical evolution and present state of conservation of Regio VII, Insula 14 in Pompeii. *Proceedings of the joint international event 9th ARQUEOLÓGICA 2.0 & 3rd GEORES*.

CloudCompare, ver. 2.11.3, 2022. <http://www.cloudcompare.org/>, last accessed 25 April 2022.

Francolini, C., Girelli, V., Bitelli, G., 2020. 3D image-based surveying of the safe of the Obellio Firmo Domus in Pompeii. *The International Archives of the Photogrammetry, Remote Sensing and Spatial Information Sciences*, XLIII-B2-2020, 1389–1394. <https://doi.org/10.5194/isprs-archives-XLIII-B2-2020-1389-2020>.

Gagliolo, S., 2021. Photogrammetric suite to manage the survey workflow in challenging environments and conditions. PhD thesis dissertation, University of Genoa, Genoa, Italy.

Gagliolo, S., Federici, B., Ferrando, I., Sguerso, D., 2019a. MAGO: a new approach for orthophotos production based on adaptive mesh reconstruction. *The International Archives of the Photogrammetry, Remote Sensing and Spatial Information Sciences*, XLII-2/W11, 533–538. <https://doi.org/10.5194/isprs-archives-XLII-2-W11-533-2019>.

Gagliolo, S., Passoni, D., Federici, B., Ferrando, I., Sguerso, D., 2019b. U.Ph.O and MAGO: two useful instruments in support of photogrammetric UAV survey. *The International Archives of the Photogrammetry, Remote Sensing and Spatial Information Sciences*, XLII-2/W13, 289–296. <https://doi.org/10.5194/isprs-archives-XLII-2-W13-289-2019>.

Girelli, V. A., Tini, M. A., Dellapasqua, M., Bitelli, G., 2019. High resolution 3D acquisition in cultural heritage knowledge and restoration projects: the survey of the fountain of Neptune in Bologna. *The International Archives of the Photogrammetry, Remote Sensing and Spatial Information Sciences*, XLII-2/W11, 573–578. <https://doi.org/10.5194/isprs-archives-XLII-2-W11-573-2019>.

Lague, D., Brodu, N., Leroux, J., 2013. Accurate 3D comparison of complex topography with terrestrial laser scanner: Application to the Rangitikei canyon (N-Z). *ISPRS journal of photogrammetry and remote sensing*, 82, 10–26. <https://doi.org/10.1016/j.isprsjprs.2013.04.009>.

Monego, M., Menin, A., Fabris, M., Achilli, V., 2019. 3D survey of Sarno Baths (Pompeii) by integrated geomatic methodologies. *Journal of Cultural Heritage*, 40, 240–246. <https://doi.org/10.1016/j.culher.2019.04.013>.

QGIS Development Team, 2022. Qgis geographic information system. <https://www.qgis.org>, last accessed on 25 April 2022.

Rupnik, E., Daakir, M., Pierrot Deseilligny, M., 2017. MicMac – a free, open-source solution for photogrammetry. *Open Geospatial Data, Software and Standards*, 2(14), 47–56. <https://doi.org/10.1186/s40965-017-0027-2>.

Tsiafaki, D., Michailidou, N., 2015. Benefits and problems through the application of 3D technologies in archaeology: recording, visualization, representation and reconstruction. <https://doi.org/10.5281/zenodo.18448>.

Verde, D., 2020. Vaulted structures in the archaeological park of Pompeii: 3D survey and monitoring. *The International Archives of the Photogrammetry, Remote Sensing and Spatial Information Sciences*, XLIV-M-1-2020, 303–309. <https://doi.org/10.5194/isprs-archives-XLIV-M-1-2020-303-2020>.